

The endosymbiont *Spiroplasma poulsonii* increases *Drosophila melanogaster* resistance to pathogens by enhancing iron sequestration and melanization

Alexandra Hrdina,^{1,2} Marina Serra Canales,¹ Aranzazu Arias-Rojas,^{1,3} Dagmar Frahm,¹ Igor Iatsenko¹

AUTHOR AFFILIATIONS See affiliation list on p. 16.

ABSTRACT Facultative endosymbiotic bacteria, such as *Wolbachia* and *Spiroplasma* species, are commonly found in association with insects and can dramatically alter their host physiology. Many endosymbionts are defensive and protect their hosts against parasites or pathogens. Despite the widespread nature of defensive insect symbioses and their importance for the ecology and evolution of insects, the mechanisms of symbiont-mediated host protection remain poorly characterized. Here, we utilized the fruit fly *Drosophila melanogaster* and its facultative endosymbiont *Spiroplasma poulsonii* to characterize the mechanisms underlying symbiont-mediated host protection against bacterial and fungal pathogens. Our results indicate a variable effect of *S. poulsonii* on infection outcome, with endosymbiont-harboring flies being more resistant to *Rhizopus oryzae*, *Staphylococcus aureus*, and *Providencia alcalifaciens* but more sensitive or as sensitive as endosymbiont-free flies to the infections with *Pseudomonas* species. Further focusing on the protective effect, we identified Transferrin-mediated iron sequestration induced by *Spiroplasma* as being crucial for the defense against *R. oryzae* and *P. alcalifaciens*. In the case of *S. aureus*, enhanced melanization in *Spiroplasma*-harboring flies plays a major role in protection. Both iron sequestration and melanization induced by *Spiroplasma* require the host immune sensor protease Persephone, suggesting a role of proteases secreted by the symbiont in the activation of host defense reactions. Hence, our work reveals a broader defensive range of *Spiroplasma* than previously appreciated and adds nutritional immunity and melanization to the defensive arsenal of symbionts.

IMPORTANCE Defensive endosymbiotic bacteria conferring protection to their hosts against parasites and pathogens are widespread in insect populations. However, the mechanisms by which most symbionts confer protection are not fully understood. Here, we studied the mechanisms of protection against bacterial and fungal pathogens mediated by the *Drosophila melanogaster* endosymbiont *Spiroplasma poulsonii*. We demonstrate that besides the previously described protection against wasps and nematodes, *Spiroplasma* also confers increased resistance to pathogenic bacteria and fungi. We identified *Spiroplasma*-induced iron sequestration and melanization as key defense mechanisms. Our work broadens the known defense spectrum of *Spiroplasma* and reveals a previously unappreciated role of melanization and iron sequestration in endosymbiont-mediated host protection. We propose that the mechanisms we have identified here may be of broader significance and could apply to other endosymbionts, particularly to *Wolbachia*, and potentially explain their protective properties.

KEYWORDS *Spiroplasma poulsonii*, endosymbionts, *Drosophila*, immune priming, host defense, pathogens

Editor Martin Kaltenpoth, Max Planck Institute for Chemical Ecology, Jena, Germany

Address correspondence to Igor Iatsenko, iatsenko@mpiib-berlin.mpg.de.

Alexandra Hrdina and Marina Serra Canales contributed equally to this article. Author order was determined on the basis of seniority.

The authors declare no conflict of interest.

See the funding table on p. 17.

Received 28 March 2024

Accepted 28 May 2024

Published 28 June 2024

Copyright © 2024 Hrdina et al. This is an open-access article distributed under the terms of the [Creative Commons Attribution 4.0 International license](https://creativecommons.org/licenses/by/4.0/).

Bacterial endosymbionts that live inside the host are commonly observed in insects (1). These endosymbionts are vertically transmitted from the mothers to their offspring, often in the egg cytoplasm. Some endosymbionts are obligate as they are essential for host development and survival by providing essential vitamins or amino acids, for example. Other endosymbionts are facultative as they are not necessary for host survival. While obligate endosymbionts reach 100% prevalence in the host insect populations, facultative endosymbionts are usually found at variable prevalence but still remain widespread in insect populations (2–4). This is because facultative endosymbionts likely have established additional approaches to increase their transmission, such as manipulating host reproduction (e.g., male killing, parthenogenesis induction, or cytoplasmic incompatibility) (5). Some facultative endosymbionts also bring ecological advantages to their hosts, such as tolerance to heat (6) or protection against natural enemies (7–9), which also contributes to the maintenance and spread of symbionts in insect populations (10–12). Symbiont-mediated defense has been confirmed in diverse insects, protecting them against a variety of antagonists, like RNA viruses, nematodes, parasitic wasps, and pathogenic fungi (9, 10, 13–19). The fact that taxonomically different symbionts can provide protection against various parasites suggests that the defensive nature of insect-microbe symbiosis is a common, if not predominant, aspect of insect symbioses.

Despite the widespread nature of defensive insect symbioses and their potential use in controlling human diseases that are vectored by insects (1, 14, 20), the mechanisms of symbiont-mediated host protection remain poorly characterized. However, the following mechanisms have been proposed. First, symbionts can improve the overall fitness of their host, for example, by providing vitamins or amino acids, thereby increasing the amount of resources the host can allocate to defense (21, 22). Second, defensive microbes can produce toxins and bioactive compounds that directly target the parasites and pathogens infecting the host. For example, the aphid symbiont *Hamiltonella defensa* protects the host from parasitoid wasps by toxins produced by a bacteriophage associated with *Hamiltonella* (23). Similarly, ribosome-inactivating-protein (RIP) toxins produced by the bacterial endosymbiont *Spiroplasma* are involved in the protection of *Drosophila* against parasitic nematodes and parasitoid wasps (19, 24, 25). Many of the symbiont-produced toxins affect essential eukaryotic processes; therefore, it is not fully understood how these toxins specifically target parasites and lack toxicity to the insect host (26). Third, microbial symbionts can competitively exclude pathogens and parasites, thereby protecting their host. This is often mediated by competition for a shared and limited resource within a host, thus limiting parasite growth. For example, *Wolbachia*'s defense against viruses in *Drosophila* may be due to the competition for cholesterol (27). Additionally, competition for host lipids has been suggested to play a role in the *Spiroplasma*-mediated protection against parasitoid wasps in *Drosophila* (28). Finally, symbiotic microorganisms can enhance host resistance against pathogens and parasites by stimulating or priming the host's immune system (29). This mechanism has been suggested to mediate the host protection by *Wolbachia* against viruses and certain bacteria (18, 30) and potentially against fungi (17). Some studies indicated that *Spiroplasma* may also induce immune responses in fruit flies, particularly the Toll pathway (19, 31). However, the significance of this immune upregulation for host defense has not been tested.

In this study, we investigated whether the endosymbiont *Spiroplasma* protects fruit flies from bacterial and fungal infections and the mechanisms that might play a role in this protection.

Along with *Wolbachia*, diverse *Spiroplasma* species are the only facultative inherited endosymbionts naturally infecting *Drosophila* flies (2, 32). Particularly, *Spiroplasma poulsonii* MSRO (melanogaster sex ratio organism) has been the focus of recent studies. It is a helical-shaped bacterium without a cell wall that lives in the hemolymph of flies, where it relies on lipids for proliferation (33, 34). *S. poulsonii* is inherited vertically through transovarial transfer (35) and causes reproductive manipulation (male killing), whereby

the sons of *S. poulsonii*-infected females are selectively killed during development. The secreted toxin *SpAID* (36, 37), which targets the dosage compensation machinery on the male X chromosome leading to apoptosis, was identified as the major male-killing factor. The genome of *S. poulsonii* MSRO was sequenced and provided the first insights into the endosymbiotic lifestyle of the bacterium (38). However, since *S. poulsonii* has been considered not cultivable *in vitro* and genetically intractable, bacterial determinants involved in host interactions remain mostly unknown. The recent development of a culture medium for *Spiroplasma in vitro* growth (39) along with the first successful transformation (40) opens the potential for genetic manipulation and functional studies of the symbiont. *S. poulsonii* is also known to protect *Drosophila* from nematodes and parasitoid wasps (15, 24, 25). This protection is achieved by metabolic competition with wasps (28) and by producing RIP toxins active against wasps and nematodes (24, 25). Previous studies, however, have not observed any protective effect of *S. poulsonii* against bacterial or fungal pathogens (41, 42). Yet, considering the limited range of previously tested pathogens, the full defensive potential of *Spiroplasma* remains to be explored. Moreover, recent findings that *Spiroplasma* induces several defense reactions in flies, such as the activation of the Toll immune pathway and iron sequestration (31, 43), led us to revise the defensive role of this symbiont.

In this study, we showed variable effects of *S. poulsonii* on infection outcomes, ranging from protective and neutral to detrimental, depending on the pathogen. Further focusing on the protective effect, we identified that iron sequestration induced by *Spiroplasma* is crucial for the defense against *Rhizopus oryzae* and *Providencia alcalifaciens*. In the case of *Staphylococcus aureus*, enhanced melanization in *Spiroplasma*-harboring flies plays a major role in protection. Both iron sequestration and melanization induced by *Spiroplasma* require the immune sensor protease Persephone, implying the role of proteases secreted by the symbiont in the activation of defense reactions. Altogether, our work adds immune priming to the previously known defense mechanisms conferred by *Spiroplasma*.

RESULTS

Spiroplasma poulsonii confers increased resistance against some pathogens

Given the lack of knowledge on the protective effect of *Spiroplasma* against bacterial and fungal pathogens, we wanted to investigate whether *Spiroplasma* affects infection outcomes with these pathogens in *D. melanogaster*. To do this, we used a wild-type (*Oregon R*) stock harboring the *Spiroplasma poulsonii* MSRO strain (Spiro+) and *Oregon R* flies without the symbiont (Spiro-) as a control (42). We infected 10-day-old, mated Spiro+ and Spiro- females with a variety of pathogens and monitored their survival. *Spiroplasma*-harboring flies survived significantly longer after infections with *S. aureus* (Fig. 1A), *R. oryzae* (Fig. 1B), and *P. alcalifaciens* (Fig. 1C) compared to control flies without *Spiroplasma*, demonstrating that *Spiroplasma* provides protection to flies against different groups of pathogens, including Gram-positive and Gram-negative bacteria and fungi. To explore whether this protection is mediated by resistance or tolerance mechanisms, we quantified the within-host burden for *R. oryzae* and *S. aureus*. Figure 1D shows that while there was no difference in *R. oryzae* load between Spiro+ and Spiro- flies at 20 h post-infection, the pathogen load was significantly reduced in Spiro+ flies compared to Spiro- flies at 40 h post-infection. The *bomanins*-deficient mutant, used as an immunocompromised control with known susceptibility to fungal infections (44), contained the highest *R. oryzae* burden among the tested flies at both time points after infection (Fig. 1D). Similarly, *S. aureus* burden was significantly lower in Spiro+ flies compared to Spiro- flies at 20 h post-infection (Fig. S1). These results suggest that Spiro+ are better than Spiro- flies at controlling pathogen growth, consistent with increased resistance rather than tolerance. Infections with the additional pathogens demonstrated that *Spiroplasma*-harboring flies are not generally more resistant to all pathogens. For example, *Spiroplasma* had no effect on the susceptibility of the flies to the versatile pathogen *Pseudomonas aeruginosa* (Fig. 1E), and the presence of the endosymbiont was

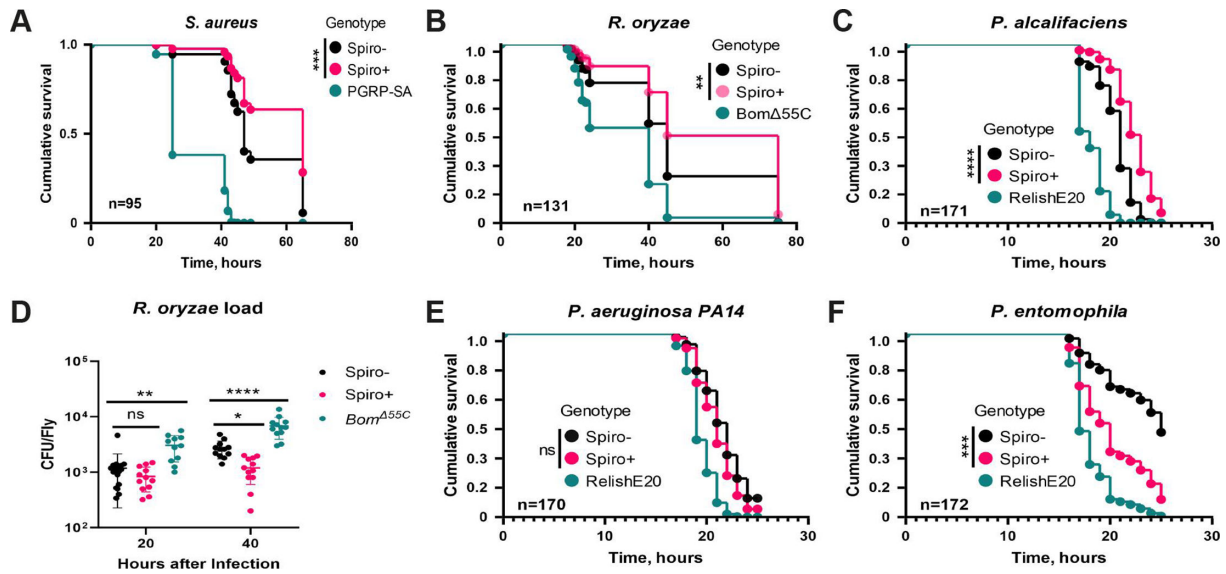


FIG 1 *Spiroplasma* has varied impact on infection outcome. (A–C) Survival rates of *Spiroplasma*-free (Spiro–) and *Spiroplasma*-harboring (Spiro+) *Oregon R* flies after infection with *S. aureus* (A), *R. oryzae* (B), and *P. alcalifaciens* (C). Toll pathway (*PGRP-SA^{SemI}* and *Bom^{Δ55C}*) and Imd pathway (*Relish^{E20}*) mutants were used as immunocompromised controls. (D) Measurement of *R. oryzae* burden at 20 and 40 h post-infection in Spiro–, Spiro+, and *Bom^{Δ55C}* flies. For CFU counts, each dot represents CFU from a pool of five animals, calculated per fly. The mean and SD are shown. (E and F) Survival rates of Spiro–, Spiro+, and *Relish^{E20}* flies after infection with *P. aeruginosa* (E) and *P. entomophila* (F). *n* = total number of flies in experiments. Asterisks indicate statistical significance. **P* ≤ 0.05; ***P* ≤ 0.01; ****P* ≤ 0.001; *****P* ≤ 0.0001; and ns, nonsignificant, *P* > 0.05.

even detrimental in the case of natural fly pathogen *Pseudomonas entomophila* (Fig. 1F). Overall, these results demonstrate that the effect of *Spiroplasma* on infection outcome is variable and could be protective, neutral, or detrimental depending on the pathogen.

We decided to further explore the bases of the protective mechanism of *Spiroplasma*. Specifically, we tested how fly age and mating status, two parameters with a known link to immunity, affect the *Spiroplasma*-conferred protection against *S. aureus*. First, we checked the effect of mating status by comparing virgin and mated 10-day-old females. Since *Spiroplasma*-harboring flies were previously shown to produce more eggs compared to symbiont-free flies (34), we hypothesized that high investment in reproduction of Spiro+ flies could reduce their ability to fight infection, consistent with the reproduction-immunity trade-off hypothesis (45). As expected, virgin flies both Spiro+ and Spiro– were more resistant to *S. aureus* infection (Fig. S2A). *Spiroplasma*-harboring flies, both mated and virgin, survived significantly longer compared to control flies without *Spiroplasma*. However, the protective effect of *Spiroplasma* in mated flies was not as strong as in virgins as illustrated by the differences in survival curves (Fig. S2A). Hence, mating reduces the protective effect of *Spiroplasma*.

When we tested the effect of age by comparing the survival of mated flies of different ages, we observed the presence of *Spiroplasma*-conferred protection in all age groups (3-, 10-, and 20-day old) that we tested (Fig. S2B). While 20-day-old flies were more susceptible to infection compared to young flies independently of endosymbiont presence, *Spiroplasma* still conferred protection to old flies, albeit to a lesser extent compared to young flies (Fig. S2B). Next, we estimated the effect of age and mating on *Spiroplasma* abundance which could affect the degree of protection. *Spiroplasma* load increased with fly age, and virgin flies harbored significantly lower symbiont quantities compared to mated flies of the same age (Fig. S2C). Despite lower *Spiroplasma* load, virgin flies survived significantly longer after *S. aureus* infection compared to mated flies. Also, while 10-day-old flies had significantly more *Spiroplasma* compared to 3-day-old flies, there was no significant difference between the two groups in the survival after *S. aureus* infection. Likewise, while 20-day-old flies had the highest *Spiroplasma* load,

they were the most susceptible to *S. aureus* infection. Overall, these results indicate that the degree of protection does not correlate with *Spiroplasma* abundance. To avoid detrimental effects of aging in old flies and immaturity of young flies, we used mated 10-day-old flies for all subsequent experiments.

Spiroplasma induces a basal level of Toll pathway activation

To gain more insights into the mechanisms underlying the *Spiroplasma*-mediated protection against pathogens, we compared differences in gene expression between 10-day-old uninfected Spiro+ and Spiro- females using RNA sequencing. We identified 22 genes with statistically significant differences in expression between Spiro+ and Spiro- flies (Fig. 2A; Table S1). Among these 22 genes, 20 were expressed at a higher level and 2 were repressed in *Spiroplasma*-harboring flies. Among induced transcripts, we noticed multiple genes linked to the Toll pathway, including serine proteases (*SPH93* and *CG33462*), *gnbp-like 3*, and several effectors of the Toll pathway (*Bomanins*, *Daishos*, and *Bombardier*) (Fig. 2A; Table S1), suggesting that *Spiroplasma* induces an immune response and specifically the Toll pathway in flies. In agreement with this, gene ontology (GO) analysis of the genes upregulated in Spiro+ flies showed enrichment of GO terms related to the defense response and the humoral immune response (Fig. S3). Similarly, serine-type endopeptidase molecular function (Fig. S3) was another identified GO term with a link to the Toll pathway due to the known role of serine proteases in the regulation of the Toll pathway. *Transferrin 1* (*tsf1*), an iron transporter with an important immune role (46, 47), was also upregulated in Spiro+ flies (Fig. 2A). Next, we tested whether infection-induced Toll pathway activation in Spiro+ flies is also stronger similarly to the basal uninfected condition. Using RT-qPCR, we confirmed a higher expression of two Toll pathway-controlled genes, *gnbp-like3* and *tsf1*, in uninfected Spiro+ compared to Spiro- flies (Fig. 2B and C). Both genes were potently induced 6 and 16 h after infection with *S. aureus* with no significant difference between Spiro+ and Spiro- flies. These results illustrate that *Spiroplasma* elicits mild (as compared to infection) Toll pathway activation under basal conditions and has no effect on the infection-induced level of Toll pathway activity. Importantly, Imd pathway activation, as measured by *dpt* expression, both at basal level and after infection with *P. alcalifaciens* was not affected by *Spiroplasma* (Fig.

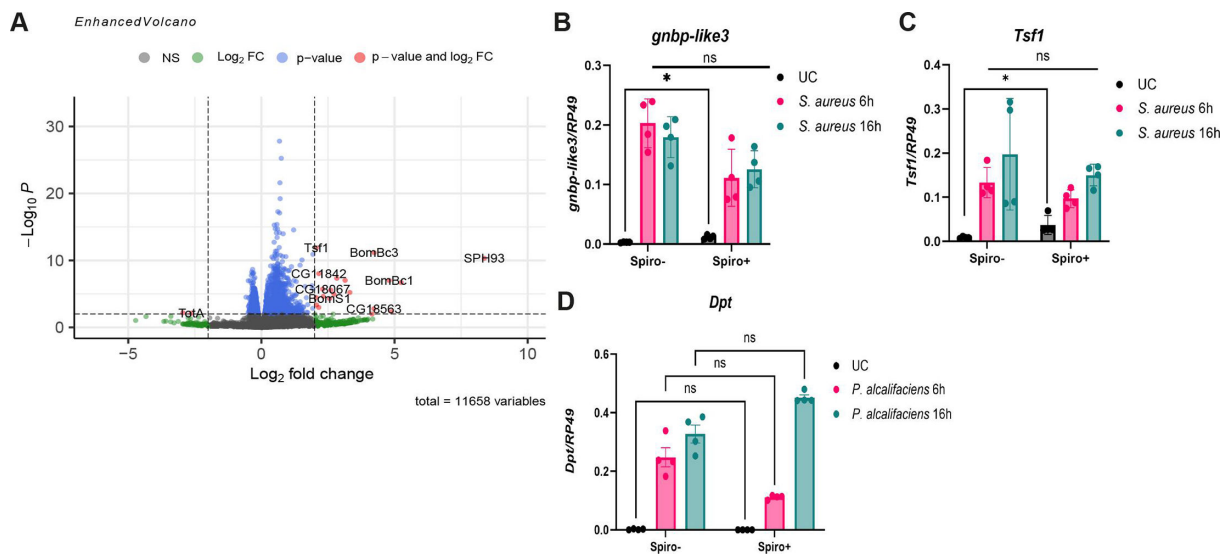


FIG 2 *Spiroplasma* induces mild Toll pathway activation. (A) Enhanced volcano plot of differentially expressed genes. The log2 fold change indicates the differential expression of genes in the *Spiroplasma*-harboring (Spiro+) versus *Spiroplasma*-free (Spiro-) samples. Red dots indicate significance as defined by an absolute fold change value over 2 or under -2 and a *P*-value below 0.05. (B–D) RT-qPCR showing *gnbp-like3* (B) and *tsf1* (C) expression in uninfected (UC) and *S. aureus*-infected Spiro- and Spiro+ flies. (D) *Diptericin A* expression in uninfected and *P. alcalifaciens*-infected Spiro- and Spiro+ flies measured by RT-qPCR. The mean and SD of four independent experiments are shown.

2D), suggesting that the increased resistance of Spiro+ flies to infections is not due to increased Imd pathway activity.

Spiroplasma-induced iron sequestration via Tsf1 contributes to the protective effect

Given a previously described role of *Tsf1*-mediated iron sequestration in the *Drosophila* defense against pathogens (46), we hypothesized that increased *tsf1* expression and iron sequestration in Spiro+ flies might be part of the defense mechanism provided by *Spiroplasma*. To test this hypothesis, we first compared the iron sequestration ability in Spiro- and Spiro+ flies by measuring iron levels in the hemolymph using a ferrozine assay. Consistent with a previous report (43), we observed significantly lower iron levels in the hemolymph of *Spiroplasma*-harboring flies relative to symbiont-free controls under basal conditions (without infection) (Fig. 3A). We confirmed this result with an additional method—inductively coupled plasma optical emission spectroscopy (ICP-OES). Importantly, while *P. alcalifaciens* infection triggered a significant drop in the hemolymph iron levels in Spiro- flies compared to uninfected controls, there was no further decrease in the amount of iron after infection in Spiro+ flies (Fig. 3A). We observed a similar result with a non-lethal pathogen *Ecc15* and with *P. entomophila*, a pathogen against which *Spiroplasma* does not provide protection (Fig. S4). These results demonstrate that *Spiroplasma* induces iron sequestration from the hemolymph

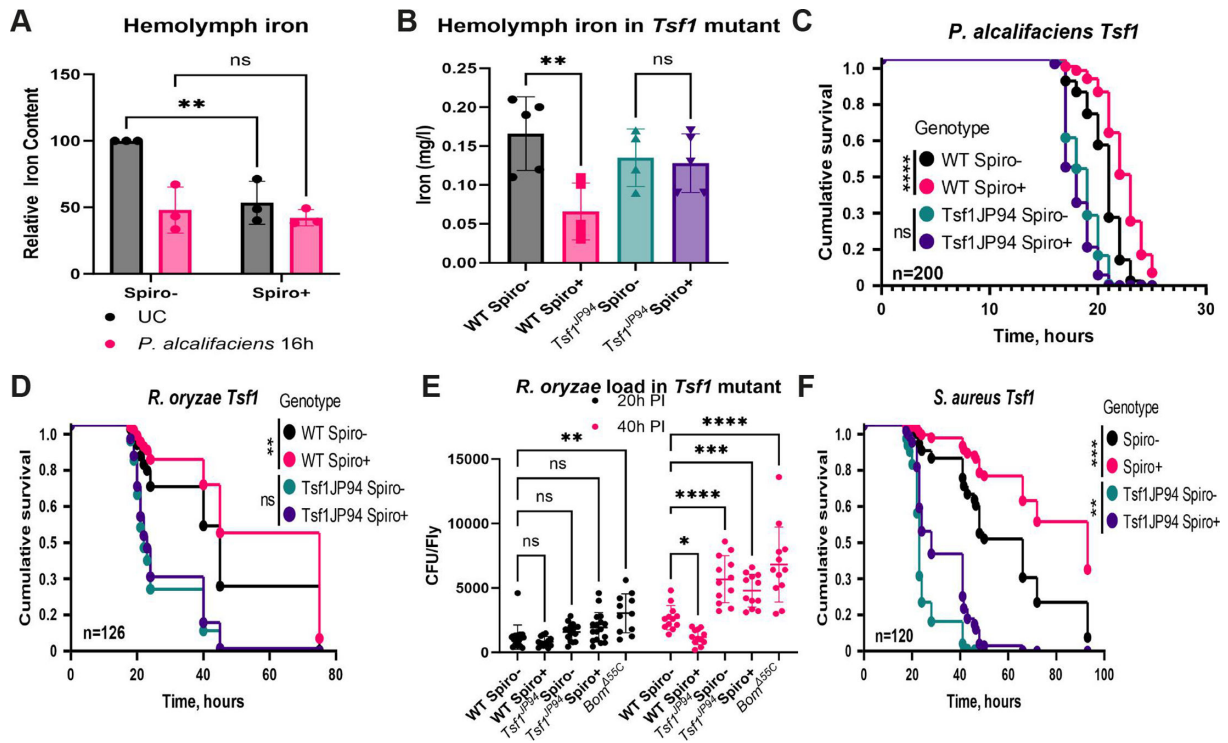


FIG 3 *Spiroplasma*-induced iron sequestration increases *Drosophila* resistance to infection. (A) Iron content of hemolymph in Spiro- and Spiro+ uninfected flies and 16 h after *P. alcalifaciens* infection measured by the ferrozine assay. Iron content in uninfected Spiro- flies was set to 100 and all other values were expressed as a percentage of this value. The mean and SD of three independent experiments are shown. (B) Hemolymph iron content in uninfected *Spiroplasma*-free (Spiro-) and *Spiroplasma*-harboring (Spiro+) wild-type (w^{1118} iso) and *Tsf1*^{JP94} iso mutant flies measured by ICP-OES. The mean and SD of four independent experiments are shown. (C and D) Survival rates of *Spiroplasma*-free (Spiro-) and *Spiroplasma*-harboring (Spiro+) wild-type (w^{1118} iso) and *Tsf1*^{JP94} iso mutant flies after infection with *P. alcalifaciens* (C) and *R. oryzae* (D). (E) Measurement of *R. oryzae* burden at 20 and 40 h post-infection in *Spiroplasma*-free (Spiro-) and *Spiroplasma*-harboring (Spiro+) wild-type (w^{1118} iso) and *Tsf1*^{JP94} iso mutant flies. For CFU counts, each dot represents CFU from a pool of five animals, calculated per fly. The mean and SD are shown. (F) Survival rates of *Spiroplasma*-free (Spiro-) and *Spiroplasma*-harboring (Spiro+) wild-type (w^{1118} iso) and *Tsf1*^{JP94} iso mutant flies after infection with *S. aureus*. *n* = total number of flies in experiments. Asterisks indicate statistical significance. **P* ≤ 0.05; ***P* ≤ 0.01; ****P* ≤ 0.001; *****P* ≤ 0.0001; and ns, nonsignificant, *P* > 0.05.

already under basal conditions. This hypoferremic response is comparable to the one induced by pathogens but is not further enhanced by the pathogens, suggesting that *Spiroplasma* and pathogens trigger iron sequestration via the same mechanism. To confirm that this mechanism involves *Tsf1*, we measured iron in the hemolymph of *Tsf1*-deficient flies colonized or not with *Spiroplasma*. Indeed, in contrast to wild-type flies, *Tsf1* mutants harboring *Spiroplasma* contained the same quantity of iron in the hemolymph as the mutant without the symbiont, indicating that *Spiroplasma*-induced sequestration is dependent on *Tsf1* (Fig. 3B). Next, we investigated whether *Tsf1* is also required for *Spiroplasma*-mediated protection against pathogens. As expected from previous studies (46, 48), *Tsf1* mutant flies were more susceptible to pathogens and had a higher pathogen load (Fig. 3C through E). While wild-type Spiro+ flies survived significantly longer compared to Spiro– flies after infections with *P. alcalifaciens* (Fig. 3C) and *R. oryzae* (Fig. 3D), we did not detect any significant effect of *Spiroplasma* on the survival of *Tsf1* mutants after infections with these pathogens. Consistent with survival, the *R. oryzae* burden was significantly higher in *Tsf1* mutants compared to wild-type flies 40 h post-infection, and *Spiroplasma* presence had no effect on the pathogen load in the *Tsf1* mutant in contrast to the inhibitory effect observed in wild-type flies (Fig. 3E). Hence, functional *Tsf1* is required for *Spiroplasma* to increase the resistance of flies to pathogens. Interestingly, when we tested the role of *Tsf1* in *Spiroplasma*-mediated protection against *S. aureus*, we observed that the protective effect in the *Tsf1* mutant was still present (Fig. 3F) since the *Spiroplasma*-harboring *Tsf1* mutant survived longer after infection compared to the Spiro– *Tsf1* mutant, although the degree of protection was not as strong as in wild-type flies. This result suggests that while *Tsf1* is partially required for *Spiroplasma*-mediated protection against *S. aureus*, it is likely that there are additional mechanisms involved.

Spiroplasma*-induced melanization is required for protection against *S. aureus

Next, we attempted to identify the additional mechanisms elicited by *Spiroplasma* that could contribute to the better survival of endosymbiont-harboring flies after *S. aureus* infection. Being motivated by a previous study (31) that identified an enrichment of melanization-related proteins in the hemolymph of Spiro+ flies, we decided to test whether *Spiroplasma* had an effect on the melanization response, which is a key defense reaction against *S. aureus* (49). We measured enzymatic phenoloxidase (PO) activity with an L-DOPA assay in adult hemolymph samples from wild-type Spiro– and Spiro+ flies. Under unchallenged conditions, these flies did not differ in PO activity, which was very low (Fig. 4A). *S. aureus* infection increased PO activity as expected. Spiro+ compared to Spiro– flies exhibited significantly higher PO activity after infection (Fig. 4A). This phenotype was not specific to *S. aureus* as we detected similarly elevated PO activity in Spiro+ flies after infections with *P. alcalifaciens* and *R. oryzae* regardless of the time of measurement (Fig. S5A and B). Additionally, we quantified crystal cells that store PPOs using a larva cooking assay. Given that all Spiro+ larvae are females, while the Spiro– population contains both sexes, we selected only female larvae for crystal cell quantification to account for potential sex bias in crystal cell numbers. As apparent from the representative images (Fig. 4B) and quantification analysis (Fig. 4C), Spiro+ larvae contained significantly more crystal cells compared to Spiro– larvae, which might also contribute to the elevated melanization response of Spiro+ animals. Notably, Spiro+ and Spiro– larvae are of a similar length (Fig. 4D), suggesting that the higher number of crystal cells in Spiro+ larvae is not just a consequence of a bigger size. To test whether enhanced melanization constitutes part of the *Spiroplasma*-mediated protection, we introduced *Spiroplasma* into the melanization-deficient *PPO1^{Δ,2^Δ,3^Δ}* mutant and scored its survival after *S. aureus* infection. As expected, *PPO1^{Δ,2^Δ,3^Δ}* mutant flies were more susceptible to *S. aureus* infection compared to wild-type flies (Fig. 4E). However, there was no significant difference in the survival between the Spiro+ and the Spiro– *PPO1^{Δ,2^Δ,3^Δ}* mutant in contrast to improved survival of wild-type Spiro+ flies (Fig. 4E).

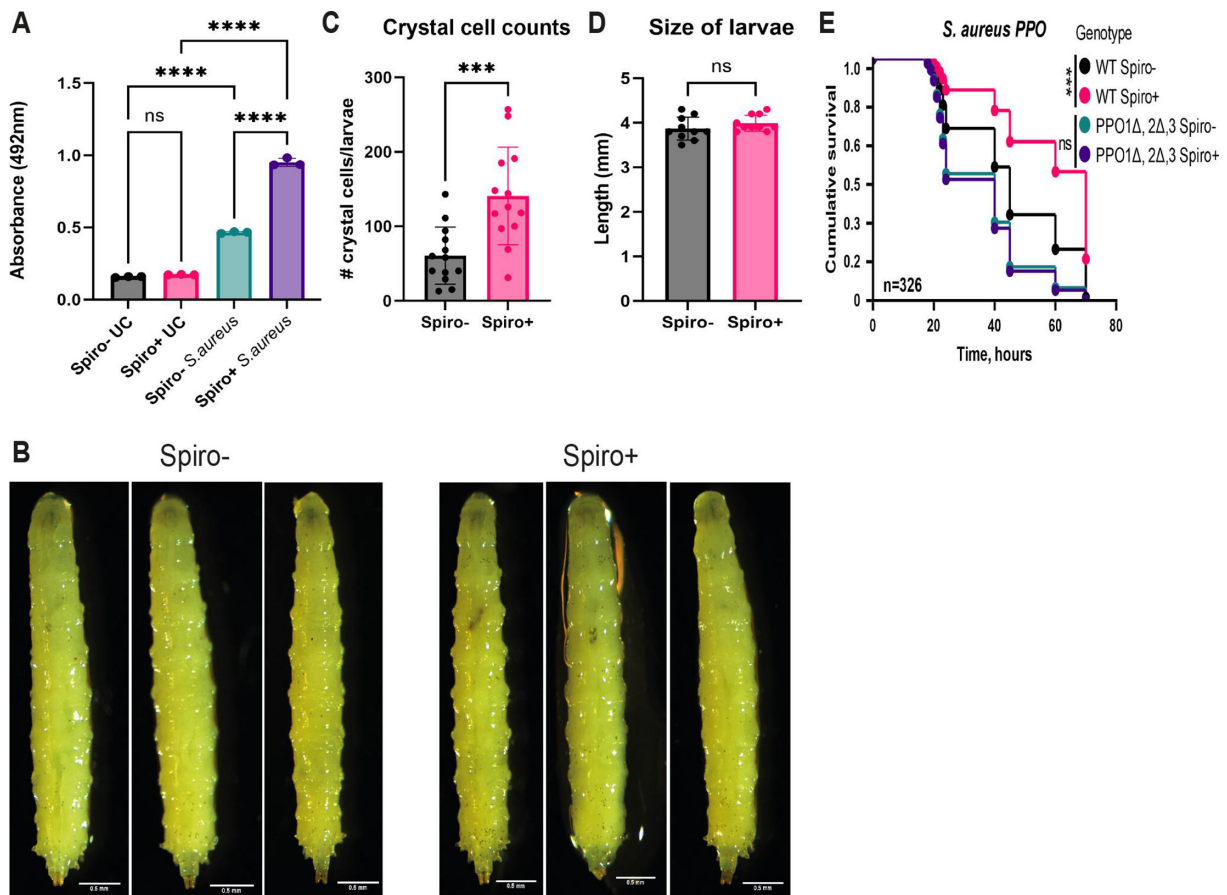


FIG 4 *Spiroplasma*-induced melanization increases *Drosophila* resistance to *S. aureus* infection. (A) Hemolymph phenoloxidase activity in uninfected flies and 3 h after *S. aureus* infection in Spiro⁻ and Spiro⁺ flies measured by the L-DOPA assay. The mean and SD of three independent experiments are shown. (B) Representative images of Spiro⁻ and Spiro⁺ *Oregon R* larvae after heat treatment (cooking assay). Scale bar is 0.5 mm. (C) Crystal cell counts in Spiro⁻ and Spiro⁺ *Oregon R* L3 stage larvae after heat treatment (cooking assay). The mean and SD are shown. (D) Length of Spiro⁻ and Spiro⁺ larvae. (E) Survival rates of *Spiroplasma*-free (Spiro⁻) and *Spiroplasma*-harboring (Spiro⁺) wild-type (w^{1118} iso) and $PPO1^{\Delta,2\Delta,3}$ iso mutant flies after infection with *S. aureus*. n = total number of flies in experiments. Asterisks indicate statistical significance. * $P \leq 0.05$; ** $P \leq 0.01$; *** $P \leq 0.001$; **** $P \leq 0.0001$; and ns, nonsignificant, $P > 0.05$.

These results suggest that a functional melanization reaction is required for *Spiroplasma* to confer protection against *S. aureus*.

Spiroplasma-mediated protection is independent of microbiota

Considering that symbionts might affect the host physiology by modulating the microbiome (50), we decided to explore whether the phenotypes of Spiro⁺ flies could be attributed to altered gut microbial communities. For this purpose, we generated axenic Spiro⁻ and Spiro⁺ flies using a standard egg bleaching protocol, which eliminates surface microbes but preserves endosymbionts. To prove that bleaching did not eliminate *Spiroplasma*, we quantified endosymbiont load, which was even slightly higher in axenic as compared to conventional flies (Fig. 5A). To confirm germ-free state of our flies, we plated fly homogenates on de Man, Rogosa, and Sharpe (MRS) and mannitol agar—media that support the growth of the majority of *Drosophila* commensals. We did not recover any bacterial colonies from axenic flies, while conventional flies, independently of *Spiroplasma* status, harbored up to 10^4 CFU per fly (Fig. 5B). Thus, *Spiroplasma* showed no effect on cultivable microbiota load, and we could successfully generate microbiota-free flies colonized with *Spiroplasma*. Next, we checked whether the phenotypes observed in conventional flies could be reproduced in axenic flies. *Spiroplasma* induced higher basal activity of the Toll pathway, as measured by *tsf1* and

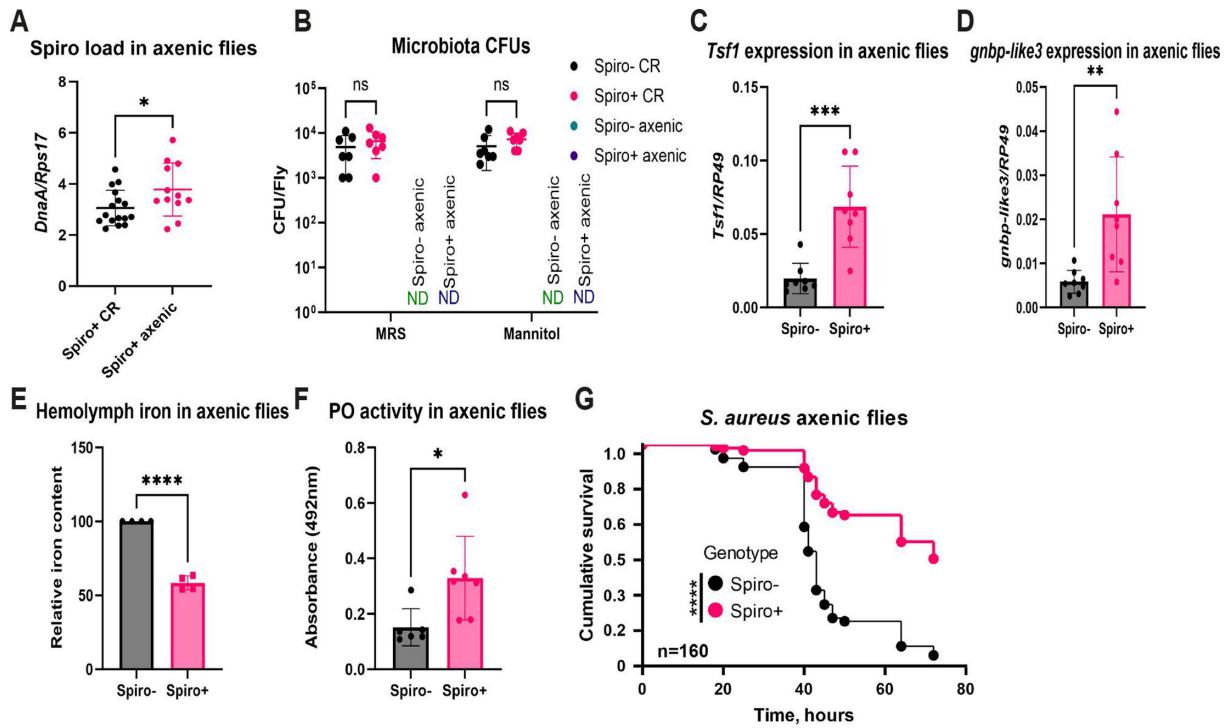


FIG 5 *Spiroplasma* confers protection independently of microbiota. (A) Quantification of *Spiroplasma* titer by RT-qPCR in axenic and conventional flies. (B) Quantification of microbiota cultivable on MRS and mannitol agar in conventional (CR) and axenic flies. Each dot represents CFU from a pool of five animals, calculated per fly. ND, not detected. The mean and SD are shown. (C and D) RT-qPCR showing *tsf1* (C) and *gnbp-like3* (D) expression in axenic Spiro– and Spiro+ flies. (E) Iron content of hemolymph in axenic Spiro– and Spiro+ flies measured by the ferrozine assay. Iron content in Spiro– flies was set to 100, and all other values were expressed as a percentage of this value. The mean and SD of four independent experiments are shown. (F) Hemolymph phenoloxidase activity measured by the L-DOPA assay in axenic Spiro– and Spiro+ flies 3 h after *S. aureus* infection. The mean and SD are shown. (G) Survival rates of *Spiroplasma*-free (Spiro–) and *Spiroplasma*-harboring (Spiro+) axenic flies after infection with *S. aureus*. *n* = total number of flies in experiments. Asterisks indicate statistical significance. **P* ≤ 0.05; ***P* ≤ 0.01; ****P* ≤ 0.001; *****P* ≤ 0.0001; and ns, nonsignificant, *P* > 0.05.

gnbp-like 3 expression (Fig. 5C and D) in axenic flies. We also observed a hypoferremic response in axenic flies characterized by significantly lower iron levels in the hemolymph of *Spiroplasma*-harboring flies relative to symbiont-free controls (Fig. 5E). Elevated PO activity after *S. aureus* infection was also preserved in Spiro+ flies under axenic conditions (Fig. 5F). Finally, *Spiroplasma* conferred protection against *S. aureus* infection (Fig. 5G) under axenic conditions too. These results illustrate that *Spiroplasma* conferred all the phenotypes under study independently of microbiota, and potential changes in the microbiome caused by the endosymbiont are unlikely to have a major contribution to the protective effect.

***Spiroplasma* induces iron sequestration and melanization via Persephone**

Finally, we wondered how *Spiroplasma* induces iron sequestration and melanization. Since both of these processes are linked to the Toll pathway, we hypothesized that their activation is a consequence of mild Toll pathway stimulation by *Spiroplasma* as supported by our RNA-seq analysis. The Toll pathway can be activated either by peptidoglycan (PGN) sensed by pattern recognition receptors (PRRs) or by secreted proteases detected by the sensor serine protease Persephone (51). Since *Spiroplasma* lacks a cell wall and PGN, detection by PRRs is unlikely. Still, to test the involvement of PRRs in the Toll pathway activation by *Spiroplasma*, we introduced the symbiont into *ModSP* mutant, which can sense proteases but is deficient in signal transmission from PRRs to the extracellular signaling cascade upstream of the Toll receptor (52). We found that the expression of the *tsf1* gene was induced by *Spiroplasma* in *ModSP* mutant

as efficiently as in wild-type flies (Fig. S6A). Also, despite increased susceptibility to *S. aureus* infection as compared to wild-type flies, *ModSP* mutant-harboring *Spiroplasma* survived significantly longer compared to symbiont-free control (Fig. S6B). These results indicate that PRRs' branch of the Toll pathway is not required for *Spiroplasma*-mediated protection and Toll pathway activation. Hence, we tested the role of protease sensing by Persephone by introducing *Spiroplasma* into a *psh* mutant and its wild-type control (*yw*). First, we measured *tsf1* gene expression by RT-qPCR in wild-type and *psh* mutant flies. While *Spiroplasma* induced on average a fourfold induction of *tsf1* in wild-type flies, in the *psh* mutant, the fold induction was close to one, indicating similar levels of *tsf1* expression in *psh* mutant flies with and without symbionts (Fig. 6A). Consistent with the lack of inducible *tsf1* expression, hemolymph iron levels were not significantly affected by *Spiroplasma* in *psh* mutant flies (Fig. 6B). Hence, *psh* is required for *Spiroplasma* to induce *tsf1* expression and iron sequestration in *Drosophila*. Similarly, in contrast to wild-type flies that exhibited increased PO activity after *S. aureus* infection in the presence of *Spiroplasma*, *psh* mutants showed only basal PO activity regardless of *Spiroplasma* status (Fig. 6C). Finally, the increased resistance to *S. aureus* infection observed in wild-type Spiro+ flies was not detected in *psh* mutants harboring *Spiroplasma* (Fig. 6D). Thus, Persephone is necessary for the *Spiroplasma*-mediated increased resistance to *S. aureus*.

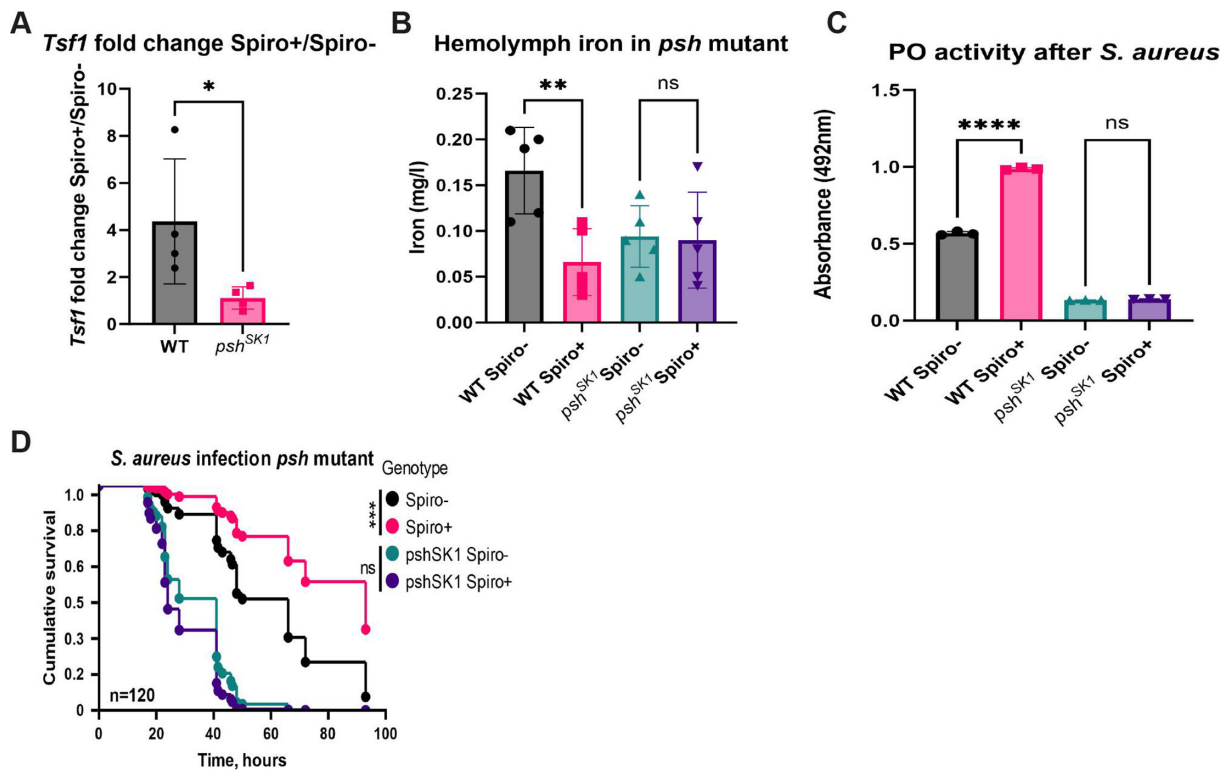


FIG 6 Persephone is required for *Spiroplasma*-induced increased resistance to pathogens. (A) RT-qPCR showing differences in the fold change of *tsf1* gene expression induced by *Spiroplasma* in wild-type and *psh*^{SK1} mutant flies. The mean and SD of four independent experiments are shown. (B) Hemolymph iron content in uninfected *Spiroplasma*-free (Spiro-) and *Spiroplasma*-harboring (Spiro+) wild-type and *psh*^{SK1} mutant flies measured by ICP-OES. The mean and SD of four independent experiments are shown. (C) Hemolymph phenoloxidase activity 3 h after *S. aureus* infection in *Spiroplasma*-free (Spiro-) and *Spiroplasma*-harboring (Spiro+) wild-type and *psh*^{SK1} mutant flies measured by the L-DOPA assay. The mean and SD of three independent experiments are shown. (D) Survival rates of *Spiroplasma*-free (Spiro-) and *Spiroplasma*-harboring (Spiro+) wild-type and *psh*^{SK1} mutant flies after infection with *S. aureus*. *n* = total number of flies in experiments. Asterisks indicate statistical significance. **P* ≤ 0.05; ***P* ≤ 0.01; ****P* ≤ 0.001; *****P* ≤ 0.0001; and ns, nonsignificant, *P* > 0.05.

DISCUSSION

The endosymbiont *Spiroplasma* has been previously shown to protect flies against wasps and nematodes (15, 25). However, *Spiroplasma's* defensive properties against other pathogens either have not been studied or were not conclusive, although there are indications that *Spiroplasma* protects aphids against fungal infections (16). Our work broadens the known defense spectrum of *Spiroplasma* and reveals a previously unappreciated role of this endosymbiont in increasing *Drosophila* resistance to bacterial and fungal pathogens. Mechanistically, this increased resistance is realized by *Spiroplasma*-induced iron sequestration and melanization. Specifically, our results support a model (Fig. 7) where proteases secreted by *Spiroplasma* are sensed by the circulating immune sensor protease Persephone, leading to the activation of the Toll pathway and the expression of *tsf1* among other effectors. Tsf1 in turn executes the iron sequestration reaction by relocating iron from the hemolymph into storage tissues, thus creating hypoferremic conditions unfavorable for pathogen growth. This iron restriction is particularly important in the defense against *P. alcalifaciens* and *R. oryzae* and only partially contributes to the defense against *S. aureus*. Additionally, *Spiroplasma*-harboring flies exhibit a Persephone-dependent excessive melanization response during infection, which is crucial for increased resistance to *S. aureus*. Thus, our work adds nutritional immunity and melanization to the defensive arsenal of symbionts. Activation of the Toll pathway by *Spiroplasma* induces other immune-responsive genes in addition to *tsf1*, including antimicrobial effectors such as *Bomanins*, which could also potentially increase the fly's resistance to fungi and Gram-positive pathogens. However, the expression of

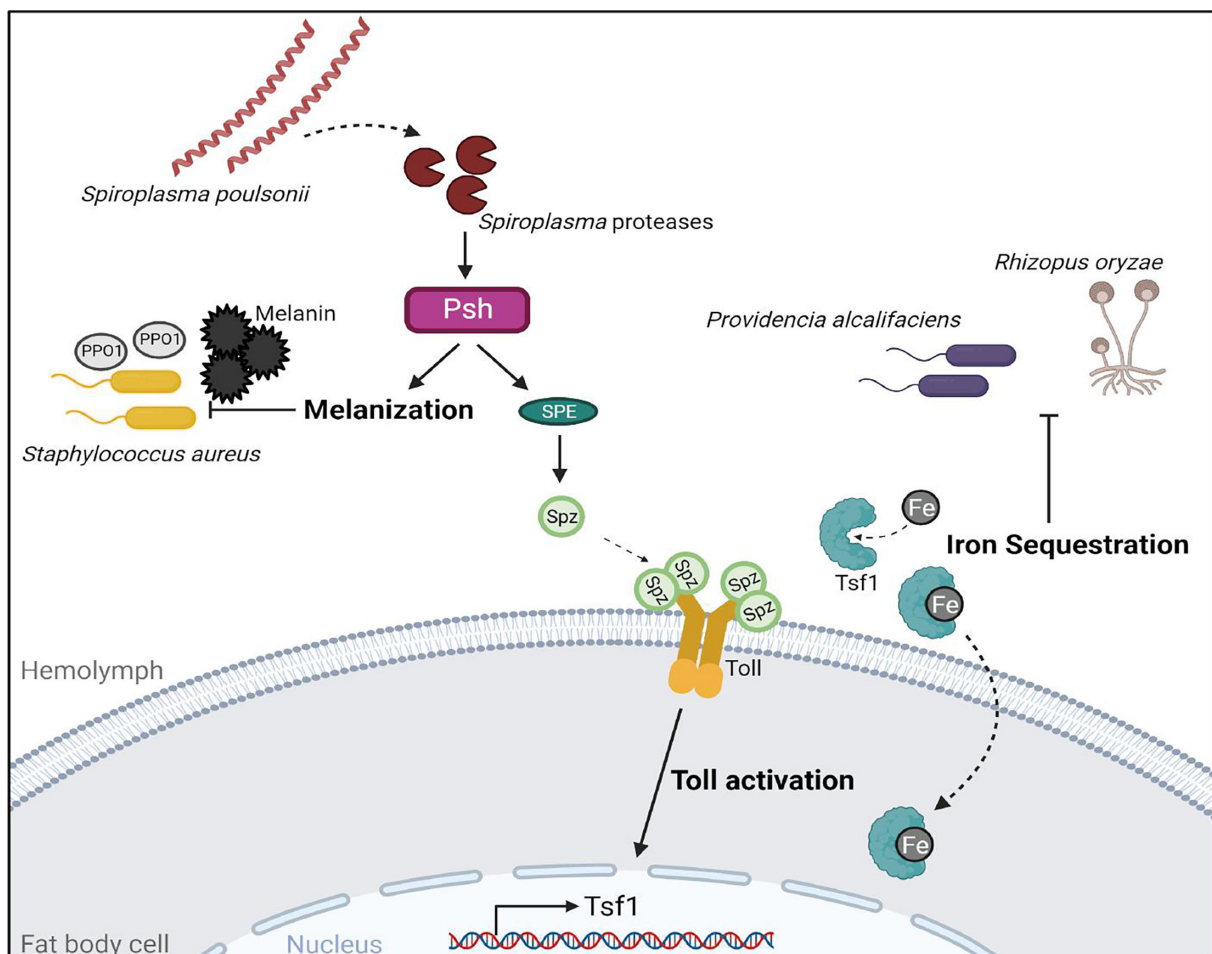


FIG 7 Graphical model illustrating the mechanisms of *Spiroplasma*-mediated host defense. See Discussion for details.

Toll pathway effectors induced by *Spiroplasma* is very low compared to infection and is therefore unlikely to be a major contributor to increased resistance. Iron sequestration on the other hand was very potently induced by *Spiroplasma* to the same level as that triggered by pathogens. In a way, *Spiroplasma*-harboring flies have a primed iron sequestration prior to infection. Thus, pathogens invading Spiro+ flies are immediately exposed to iron-restricted conditions, while in Spiro- flies, this hypoferremic response needs time to be initiated, consequently allowing the pathogens to benefit from the iron, proliferate more, and kill the host faster. While *Spiroplasma*-induced iron sequestration clearly improves the resistance of flies to pathogens, it is not known whether this chronic alteration in iron storage may have detrimental effects in the long term. For example, iron overload is known to cause tissue and organ damage (53). Therefore, we cannot exclude that the increased iron load in storage tissues (fat body) of Spiro+ flies contributes to the reduced lifespan of these flies (43). Chronic hypoferremia observed in the hemolymph of Spiro+ flies might similarly adversely affect the physiology of flies.

Previous studies that looked into gene expression changes induced by *Spiroplasma* in flies reported conflicting results. For example, RT-qPCR did not reveal a significant impact of *Spiroplasma* on the Imd and Toll pathway activation in flies (42). Studies that used RNA-seq either did not detect any upregulated genes in Spiro+ flies (54) or identified few immune genes, including *PPO1* and several serine proteases induced in *Spiroplasma*-harboring flies (19). While the nature of these discrepancies is not clear, differences in the age of flies used by various studies might be part of the explanation. Consistent with Hamilton et al. (19), our transcriptomic analysis revealed that serine proteases and several Toll pathway-regulated immune genes are induced by *Spiroplasma*. Importantly, the transcriptional changes that we detected translate into alterations at the protein level, as the corresponding proteins were enriched in the hemolymph of *Spiroplasma*-harboring flies (31). Thus, our work and the work of Masson et al. (31) challenge the assumption that *Spiroplasma* is undetectable by the immune system due to the lack of peptidoglycan, a main elicitor of the fly immune response. Instead, our results support a hypothesis that *Spiroplasma* activates the Toll pathway via the soluble sensor protease Persephone, which detects proteases released by the endosymbiont. The genome of *Spiroplasma* (38, 55) encodes at least 12 putative proteases, and 4 of them (ATP-dependent zinc metalloprotease FtsH, ATP-dependent Clp protease ATP-binding subunit ClpC, Lon protease 1, and RIP metalloprotease RseP) were detected in the fly hemolymph by proteomic analysis (31). Hence, at least some of the proteases are secreted by *Spiroplasma* into the hemolymph. Whether and which of these proteases can cleave and activate Persephone remains to be demonstrated.

In addition to iron sequestration induced by *Spiroplasma*, we observed an increased Persephone-dependent melanization response in endosymbiont-harboring flies. The fact that *Spiroplasma* could not increase the resistance of melanization-deficient flies to *S. aureus* infection illustrates the crucial role of the melanization response in the endosymbiont-mediated defense. However, the question of how *Spiroplasma* enhances the melanization response remains open. Considering the essential function of Persephone in the melanization response, one possibility could be that the activation of Persephone by *Spiroplasma*-secreted proteases triggers the melanization reaction in addition to the Toll pathway activation. However, in this scenario, we would expect constitutively higher melanization in Spiro+ flies. Our PO activity measurements illustrate that this is not the case, and Spiro+ flies have higher PO activity only after infection. This suggests that proteases secreted by *Spiroplasma* are either not sufficient to initiate the melanization reaction or that the PPOs are not accessible to proteases in the absence of injury. An alternative possibility could be that the higher number of crystal cells in Spiro+ animals results in higher PO activity. Given that crystal cells store PPOs and release them in the hemolymph only after injury, this would explain why Spiro+ flies have enhanced PO activity only after infection and not constitutively. Since the Toll pathway regulates the expression of many genes involved in melanization (56), it is very likely that basal activity of this pathway in Spiro+ flies is sufficient to promote crystal cell differentiation.

Although our results differ from those reported by Paredes et al. (28), who found no effect of *Spiroplasma* on crystal cell counts after wasp infection, they raise the need for a more detailed investigation of the impact of *Spiroplasma* on the cellular immune response.

Several prior studies that explored a potential defensive role of *Spiroplasma* against bacterial pathogens found either no effect of the endosymbiont on infection outcome or an increased susceptibility of Spiro+ flies to certain Gram-negative pathogens (41, 42). Although we used different pathogens, we also had cases with no or negative effects of *Spiroplasma* on the resistance to pathogens. What determines whether or not *Spiroplasma* is protective against a specific pathogen remains to be investigated. However, considering that *Spiroplasma* affects several processes in flies, it is possible that synergistic or antagonistic interactions between these processes and their importance in the defense against a particular pathogen play a decisive role in the infection outcome. For example, we have previously shown that melanization and the Toll pathway do not play a role in the defense against *P. alcalifaciens*, while iron sequestration is very important (48). Thus, it is very likely that the iron sequestration induced by *Spiroplasma* is a sole or very prominent defense mechanism. In the case of *S. aureus*, both melanization and iron sequestration likely contribute, but since the protection was still present in *Tsf1* but not in *PPO1^{Δ,2^Δ,3¹}* mutants, this suggests that melanization is more important in the case of *S. aureus*. However, how these two reactions interact with each other and with the other defense responses, and whether this has consequences for resistance to specific pathogens, remains to be investigated. Given the prominent role of iron sequestration in the defense against *Pseudomonas* sp. (46), it was surprising to see no increased resistance of Spiro+ flies against *P. aeruginosa* and *P. entomophila*. This result suggests that probably *Spiroplasma* affects additional processes in flies that override the protective effect of iron sequestration. For example, our RNA-seq analysis identified two JAK-STAT pathway-regulated genes, *totA* and *totM*, being repressed in Spiro+ flies. This raises the possibility that reduced JAK-STAT pathway signaling in Spiro+ flies might make them more susceptible to *P. entomophila* infection. Alternatively, reduced hemolymph iron levels in *Spiroplasma*-harboring flies might reduce the production of reactive oxygen species, which are also important immune effectors. We also cannot exclude the possibility that although melanization is an important defense reaction against *S. aureus*, it might be detrimental during *P. entomophila* infection.

Taken together, our study demonstrates a previously unrecognized defensive role of *Spiroplasma* against bacterial and fungal pathogens and identifies melanization and iron sequestration as endosymbiont-induced immune reactions mediating the protective effect.

Whether other symbionts, like *Wolbachia* (57), could similarly activate melanization and iron sequestration in insects, and whether these reactions protect insects not only from bacterial pathogens but also from nematodes and wasps, would be an interesting avenue to explore for future studies.

MATERIALS AND METHODS

Drosophila stocks and rearing

Spiroplasma poulsonii MSRO Uganda-1 strain was used in all fly stocks harboring *Spiroplasma*. Oregon R stocks uninfected and infected with *S. poulsonii* MSRO Uganda-1 were established several years prior to the current study as previously described (42). To establish additional fly stocks infected with *Spiroplasma*, 9 nL of MSRO-infected hemolymph was injected into the thorax of mated females of the stock to be infected. The progeny of these flies was collected after 5–7 days using male killing as a proxy to assess the infection (100% female progeny). The newly established *Spiroplasma*-harboring fly stocks were maintained by adding uninfected males of the same genetic background that were maintained in parallel as control stocks. Given that *Spiroplasma*-infected stocks due to male killing produce only females (around half of the total

fly population), this introduces a bias in the rearing density. To correct such bias, we put 1.5 times more *Spiroplasma*-infected than *Spiroplasma*-free females per vial, which combined with the higher amount of eggs laid by *Spiroplasma*-infected females resulted in a comparable rearing density. The following stocks used in this study were kindly provided by Bruno Lemaitre: *Bom*^{Δ55C}; *ywDD*, *PGRP-SA*^{Semi}, *Relish*^{E20} iso; *DrosDel w*¹¹¹⁸ iso; *Tsf1*^{JP94} iso; *PPO1*^{Δ,2^Δ,3¹} iso; *yw*; *yw psh*^{SK1}; *ModSP*¹ (43, 44, 48, 49, 52, 58, 59). Female flies were used in all experiments.

Drosophila stocks were kept at 25°C on a standard cornmeal-agar medium (3.72 g agar, 35.28 g cornmeal, 35.28 g inactivated dried yeast, 16 mL of a 10% solution of methyl-paraben in 85% ethanol, 36 mL fruit juice, and 2.9 mL 99% propionic acid for 600 mL). Flies were flipped to new vials with fresh food every 3–4 days to grow new generations. Axenic flies were generated by egg bleaching as previously described (59) with the exception that antibiotics were omitted from the food. Microbiota-free status of axenic flies and microbiota estimation in conventional flies were performed by plating serial dilutions of fly homogenates on MRS and mannitol agar.

Pathogen strains and survival experiments

The bacterial strains used and their respective optical densities (OD) at 600 nm were Gram-negative bacteria *Pectobacterium carotovorum* (*Ecc15*, OD₂₀₀), *P. entomophila* (OD₁), *P. aeruginosa* (PA14, OD₁), and *P. alcalifaciens* (OD₂); Gram-positive bacteria *S. aureus* (OD₁); and the fungi *R. oryzae*. Microbes were cultured in Luria broth (LB) at 29°C (*Ecc15* and *P. entomophila*) or 37°C (all others). Spores of the *R. oryzae* were grown on malt agar plates at 29°C for ~3 weeks until sporulation.

Systemic infections (septic injury) were performed by pricking adult flies in the thorax with a thin needle previously dipped into the bacterial culture or in a suspension of fungal spores. Infected flies were subsequently maintained at 25°C overnight and changed to 29°C the next morning and surviving flies were counted at regular intervals. Two or three vials of 15–20 flies were used for survival experiments, and survivals were repeated a minimum of two times.

Quantification of pathogen load

Flies were systemically infected with bacteria at the above-indicated OD and allowed to recover. At the indicated time points post-infection, flies were anesthetized using CO₂ and surface sterilized by washing them in 70% ethanol. Flies were homogenized using a Precellys Evolution Homogenizer at 7,200 rpm, 1 cycle for 30 s in 500 μL of sterile phosphate-buffered saline (PBS) for sets of five flies. These homogenates were serially diluted and plated on LB agar in 10 μL triplicates. Bacterial plates were incubated at the corresponding bacterial culture temperature overnight, and colony-forming units were counted manually.

For *R. oryzae*, PBS with 0.01% tween-20 was used instead of PBS. Serial 50 μL dilutions were spread evenly on malt agar plates and left at room temperature overnight.

The equation used to calculate CFU/fly is as follows:

$$\text{CFU/mL} = (\text{no. of colonies} \times \text{total dilution factor}) / \text{volume of culture plated in milliliters}$$
$$\text{CFU/fly} = (\text{CFU/mL}) \times \text{total volume/total flies}$$

RT-qPCR

For the quantification of messenger RNA, whole flies ($n = 10$) were collected at indicated time points. Total RNA was isolated using TRIzol reagent and dissolved in RNase-free water. A total of 500 ng of total RNA was then reverse transcribed in 10 μL reactions using PrimeScript RT (TAKARA) and random hexamer primers. The qPCR was performed on a LightCycler 480 (Roche) in 96-well plates using the SYBR Select Master Mix from Applied Biosystems. RP49 was used as a housekeeping gene for normalization. Relative expression of target transcripts was calculated following the $\Delta\Delta\text{CT}$ method (60). Primer sequences were published previously (31, 46).

***Spiroplasma* quantification**

Spiroplasma quantification was performed by qPCR as previously described (42). Briefly, the DNA was extracted from pools of five whole flies, and the copy number of a single-copy bacterial gene (*dnaA*) was quantified and normalized by that of the host gene *rsp17*. Primer sequences were published previously (42).

RNA-seq and GO analysis

Total RNA was extracted from 10 whole flies per sample using TRIzol reagent. Total RNA was dissolved in nuclease-free water, and RNA concentration was measured using a Nanodrop (Thermo Scientific). RNA integrity and quality were estimated using a Bioanalyzer (Agilent Technologies). Separate libraries for the two experimental conditions belonging to three independent experiments were prepared with the TruSeq RNA Sample Prep kit (Illumina, San Diego, CA, USA) according to the manufacturer's protocol. The DNA was purified between enzymatic reactions, and the size selection of the library was performed with AMPure XT beads (Beckman Coulter Genomics, Danvers, MA, USA). The libraries were pooled and sequenced using Illumina HiSeq 3000 instrument (75 bp paired-end sequencing) at the Max Planck-Genome-Centre Cologne, Germany (<https://mpgc.mpiiz.mpg.de/home/>).

The RNA-seq data from this study (PRJNA1051545) were analyzed using CLC Genomics Workbench (version 12.0 and CLC Genomics Server Version 11.0). The analysis involved employing the "Trim Reads" function (61) and the "RNA-Seq Analysis" tool. Mapping and read counting were performed using the BDGP6.28 Ensembl genome as the reference.

Differential expression analysis was executed through DESeq2 (62). Gene ontology analysis and GO term enrichment on gene group lists were carried out using FlyMine (63), with a background list comprising 11,659 reproducibly measured genes. The obtained results were filtered using a corrected *P*-value threshold of <0.05 (Holm-Bonferroni). To visualize the data, the R packages ggplot2, dplyr, org.Dm.eg.db, and EnhancedVolcano were employed.

Hemolymph extraction and colorimetric iron measurement

To extract hemolymph, 100 female flies that were infected for 24 h were anesthetized and placed on a 10 µm filter inside an empty Mobicol spin column (MoBiTec). Glass beads were added on top of the flies, and columns were centrifuged for 10 min at 4°C, 5,000 rpm. The collected hemolymph was used for different assays. To measure iron levels, 5–8 µL of hemolymph was collected in 50 µL of Protease Inhibitor cocktail (Sigma, Catalog #11697498001). Then, each sample was diluted in a 1:10 ratio and measured by the Pierce BCA Protein Assay Kit (Thermo Fisher Scientific) according to the manufacturer's protocol. Iron concentration in each sample was normalized to the total protein amount to standardize sample size differences, whereby 120 µg was used as the sample in each assay. Protein samples (made up to 50 µL) were hydrolyzed with 11 µL of 32% hydrochloric acid under heating conditions (95°C) for 20 min and centrifuged for 10 min at 20°C, 16,000 *g*. A volume of 18 µL of 75 mM ascorbate was added to 45 µL of supernatant followed by 18 µL of 10 mM ferrozine and 36 µL of ammonium acetate. Absorbance was measured at 562 nm using an Infinite 200 Pro plate reader (Tecan). Quantification was performed using a standard curve generated with serial dilutions of a 10 mM FAC stock dilution.

Iron measurement using inductively coupled plasma optical emission spectrometry

Hemolymph extraction was performed as described above. Then, 20 µL of hemolymph per sample was digested with 0.5 mL of 32% ultrapure hydrochloric acid (VWR Chemicals) under heating conditions (60°C) for 2 h; 9.5 mL of nitric acid was added to each

sample, and the iron quantification was performed on an ICP-OES iCAP 6300 Duo MFC (Thermo Fisher Scientific) at Humboldt University Berlin.

Crystal cell count

Third instar (L3) larvae were collected in a 1.5 mL Eppendorf tube with PBS and placed in a heat block at 67°C for 20 min. Larvae were placed on slides and melanization spots were counted manually under ZEISS Stemi 305 stereomicroscope. Pictures of melanized larvae were captured with a Leica M 210 F microscope, a Leica DMC4500 camera, and the Leica Application Suite.

PO activity

Hemolymph extraction was performed as described above. A volume of 5 μ L of hemolymph was diluted in a 1:10 ratio in 45 μ L of Protease Inhibitor cocktail. The protein concentration was adjusted after Pierce BCA Assay. Sample volumes were adjusted in 200 μ L of 5 mM CaCl_2 solution. After the addition of 800 μ L L-DOPA solution (20 mM, pH 6.6), the samples were incubated at 29°C for 20–23 h in the dark, and the OD at 492 nm was measured every 20 min. Each experiment was run in technical duplicates and repeated three times.

Quantification and statistical analysis

Data representation and statistical analysis were performed using GraphPad Prism 10 software. Each experiment was repeated independently a minimum of three times (unless otherwise indicated), and error bars represent the standard deviation (SD) of replicate experiments. The survival graphs show cumulative survival. At least two replicate survival experiments were performed for each infection, with 15–20 female flies per vial on standard fly medium without yeast. Survival results were statistically analyzed using the Cox-proportional hazard model. The normal distribution of data was checked using D'Agostino-Pearson test. Two-way ANOVA was used to analyze the data in Fig. 1D, 2B through D, 3A, B, E, 4A, and 5B; unpaired *t*-test was used to analyze the data in Fig. 4C and D 5A and C through F. Where multiple comparisons were necessary, appropriate Tukey, Dunnett, or Sidak *post hoc* tests were applied. Other details on statistical analysis can be found in figure legends. Statistical significance was set at $P \leq 0.05$. * $P \leq 0.05$; ** $P \leq 0.01$; *** $P \leq 0.001$; **** $P \leq 0.0001$; and ns, non-significant, $P > 0.05$.

ACKNOWLEDGMENTS

We are grateful to Dr. Bruno Lemaitre for the fly stocks. We thank Dr. Kirsten Weiss (Humboldt University Berlin) for technical help with the ICP-OES analysis of the iron content. We thank the Max Planck-Genome-Centre Cologne (<http://mpgc.mpipz.mpg.de/home/>) for performing the RNA-seq in this study.

I.I. acknowledges funding from the Max Planck Society and the Deutsche Forschungsgemeinschaft (DFG) grant IA 81/2-1.

AUTHOR AFFILIATIONS

¹Research group Genetics of Host-Microbe Interactions, Max Planck Institute for Infection Biology, Berlin, Germany

²Faculty of Life Sciences, Humboldt-Universität zu Berlin, Berlin, Germany

³Department of Biology, Chemistry, and Pharmacy, Freie Universität Berlin, Berlin, Germany

PRESENT ADDRESS

Marina Serra Canales, College of Medical, Veterinary & Life Sciences, School of Molecular Biosciences, University of Glasgow, Glasgow, United Kingdom

AUTHOR ORCID*s*

Igor Iatsenko  <http://orcid.org/0000-0002-9249-8998>

FUNDING

Funder	Grant(s)	Author(s)
Deutsche Forschungsgemeinschaft (DFG)	IA 81/2-1	Alexandra Hrdina Igor Iatsenko

DATA AVAILABILITY

All raw RNA sequencing data files are available from the SRA database (accession number [PRJNA1051545](https://www.ncbi.nlm.nih.gov/sra/PRJNA1051545)).

ADDITIONAL FILES

The following material is available [online](#).

Supplemental Material

Supplemental material (mBio00936-24-S0001.pdf). Fig. S1–S6.

Table S1 (mBio00936-24-S0002.csv). Genes differentially expressed between *Spiroplasma*-harboring and *Spiroplasma*-free 10-day-old *Oregon R* female flies.

REFERENCES

- Kikuchi Y. 2009. Endosymbiotic bacteria in insects: their diversity and culturability. *Microbes Environ* 24:195–204. <https://doi.org/10.1264/j sme2.me09140s>
- Mateos M, Castrezana SJ, Nankivell BJ, Estes AM, Markow TA, Moran NA. 2006. Heritable endosymbionts of *Drosophila*. *Genetics* 174:363–376. <https://doi.org/10.1534/genetics.106.058818>
- Masson F, Lemaître B. 2020. Growing ungrowable bacteria: overview and perspectives on insect symbiont culturability. *Microbiol Mol Biol Rev* 84:e00089-20. <https://doi.org/10.1128/MMBR.00089-20>
- Eleftherianos I, Atri J, Accetta J, Castillo JC. 2013. Endosymbiotic bacteria in insects: guardians of the immune system? *Front Physiol* 4:46. <https://doi.org/10.3389/fphys.2013.00046>
- Engelstädter J, Hurst GDD. 2009. The ecology and evolution of microbes that manipulate host reproduction. *Annu Rev Ecol Evol Syst* 40:127–149. <https://doi.org/10.1146/annurev.ecolsys.110308.120206>
- Montllor CB, Maxmen A, Purcell AH. 2002. Facultative bacterial endosymbionts benefit pea aphids *Acyrtosiphon pisum* under heat stress. *Ecol Entomol* 27:189–195. <https://doi.org/10.1046/j.1365-2311.2002.00393.x>
- Vorburger C, Perlman SJ. 2018. The role of defensive symbionts in host-parasite coevolution. *Biol Rev Camb Philos Soc* 93:1747–1764. <https://doi.org/10.1111/brv.12417>
- Florez LV, Biedermann PHW, Engl T, Kaltenpoth M. 2015. Defensive symbioses of animals with prokaryotic and eukaryotic microorganisms. *Nat Prod Rep* 32:904–936. <https://doi.org/10.1039/c5np00010f>
- Oliver KM, Russell JA, Moran NA, Hunter MS. 2003. Facultative bacterial symbionts in aphids confer resistance to parasitic wasps. *Proc Natl Acad Sci U S A* 100:1803–1807. <https://doi.org/10.1073/pnas.0335320100>
- Jaenike J, Unckless R, Cockburn SN, Boelio LM, Perlman SJ. 2010. Adaptation via symbiosis: recent spread of a *Drosophila* defensive symbiont. *Science* 329:212–215. <https://doi.org/10.1126/science.1188235>
- Haine ER. 2008. Symbiont-mediated protection. *Proc Biol Sci* 275:353–361. <https://doi.org/10.1098/rspb.2007.1211>
- Zhao D, Zhang Z, Niu H, Guo H. 2023. Pathogens are an important driving force for the rapid spread of symbionts in an insect host. *Nat Ecol Evol* 7:1667–1681. <https://doi.org/10.1038/s41559-023-02160-3>
- Teixeira L, Ferreira A, Ashburner M. 2008. The bacterial symbiont *Wolbachia* induces resistance to RNA viral infections in *Drosophila melanogaster*. *PLoS Biol* 6:e2. <https://doi.org/10.1371/journal.pbio.1000002>
- Moreira LA, Iturbe-Ormaetxe I, Jeffery JA, Lu G, Pyke AT, Hedges LM, Rocha BC, Hall-Mendelin S, Day A, Riegler M, Hugo LE, Johnson KN, Kay BH, McGraw EA, van den Hurk AF, Ryan PA, O'Neill SL. 2009. A *Wolbachia* symbiont in *Aedes aegypti* limits infection with dengue, chikungunya, and Plasmodium. *Cell* 139:1268–1278. <https://doi.org/10.1016/j.cell.2009.11.042>
- Xie J, Tiner B, Vilchez I, Mateos M. 2011. Effect of the *Drosophila* endosymbiont *Spiroplasma* on parasitoid wasp development and on the reproductive fitness of wasp-attacked fly survivors. *Evol Ecol* 53:1065–1079. <https://doi.org/10.1007/s10682-010-9453-7>
- Łukasik P, van Asch M, Guo H, Ferrari J, Godfray HCJ. 2013. Unrelated facultative endosymbionts protect aphids against a fungal pathogen. *Ecol Lett* 16:214–218. <https://doi.org/10.1111/ele.12031>
- Perlmutter JI, Atadurdiyeva A, Schedl ME, Unckless RL. 2023. *Wolbachia* enhances the survival of *Drosophila* infected with fungal pathogens. *bioRxiv*. <https://doi.org/10.1101/2023.09.30.560320>
- Gupta V, Vasanthakrishnan RB, Siva-Jothy J, Monteith KM, Brown SP, Vale PF. 2017. The route of infection determines *Wolbachia* antibacterial protection in *Drosophila*. *Proc R Soc B Biol Sci* 284. <https://doi.org/10.1098/rspb.2017.0809>
- Hamilton PT, Leong JS, Koop BF, Perlman SJ. 2014. Transcriptional responses in a *Drosophila* defensive symbiosis. *Mol Ecol* 23:1558–1570. <https://doi.org/10.1111/mec.12603>
- Hughes GL, Koga R, Xue P, Fukatsu T, Rasgon JL. 2011. *Wolbachia* infections are virulent and inhibit the human malaria parasite *Plasmodium falciparum* in *Anopheles gambiae*. *PLoS Pathog* 7:e1002043. <https://doi.org/10.1371/journal.ppat.1002043>
- Kanyile SN, Engl T, Kaltenpoth M. 2022. Nutritional symbionts enhance structural defence against predation and fungal infection in a grain pest beetle. *J Exp Biol* 225:jeb243593. <https://doi.org/10.1242/jeb.243593>
- Cornwallis CK, van 't Padje A, Eilers J, Klein M, Jackson R, Kiers ET, West SA, Henry LM. 2023. Symbioses shape feeding niches and diversification across insects. *Nat Ecol Evol* 7:1022–1044. <https://doi.org/10.1038/s41559-023-02058-0>
- Oliver KM, Degnan PH, Hunter MS, Moran NA. 2009. Bacteriophages encode factors required for protection in a symbiotic mutualism. *Science* 325:992–994. <https://doi.org/10.1126/science.1174463>

24. Ballinger MJ, Perlman SJ. 2017. Generality of toxins in defensive symbiosis: ribosome-inactivating proteins and defense against parasitic wasps in *Drosophila*. *PLoS Pathog* 13:e1006431. <https://doi.org/10.1371/journal.ppat.1006431>
25. Hamilton PT, Peng F, Boulanger MJ, Perlman SJ. 2016. A ribosome-inactivating protein in a *Drosophila* defensive symbiont. *Proc Natl Acad Sci U S A* 113:350–355. <https://doi.org/10.1073/pnas.1518648113>
26. Garcia-Arreaez MG, Masson F, Escobar JCP, Lemaître B. 2019. Functional analysis of RIP toxins from the *Drosophila* endosymbiont *Spiroplasma poulsonii*. *BMC Microbiol* 19:46. <https://doi.org/10.1186/s12866-019-1410-1>
27. Caragata EP, Rancès E, Hedges LM, Gofton AW, Johnson KN, O'Neill SL, McGraw EA. 2013. Dietary cholesterol modulates pathogen blocking by *Wolbachia*. *PLoS Pathog* 9:e1003459. <https://doi.org/10.1371/journal.ppat.1003459>
28. Paredes JC, Herren JK, Schüpfer F, Lemaître B. 2016. The role of lipid competition for endosymbiont-mediated protection against parasitoid wasps in *Drosophila*. *mBio* 7:e01006-16. <https://doi.org/10.1128/mBio.01006-16>
29. Hoang KL, King KC. 2022. Symbiont-mediated immune priming in animals through an evolutionary lens. *Microbiology (Reading)* 168:001181. <https://doi.org/10.1099/mic.0.001181>
30. Kambris Z, Blagborough AM, Pinto SB, Blagrove MSC, Godfray HCJ, Sinden RE, Sinkins SP. 2010. *Wolbachia* stimulates immune gene expression and inhibits Plasmodium development in *Anopheles gambiae*. *PLoS Pathog* 6:e1001143. <https://doi.org/10.1371/journal.ppat.1001143>
31. Masson F, Rommelaere S, Marra A, Schüpfer F, Lemaître B. 2021. Dual proteomics of *Drosophila melanogaster* hemolymph infected with the heritable endosymbiont *Spiroplasma poulsonii*. *PLoS One* 16:e0250524. <https://doi.org/10.1371/journal.pone.0250524>
32. Haselkorn TS, Markow TA, Moran NA. 2009. Multiple introductions of the *Spiroplasma* bacterial endosymbiont into *Drosophila*. *Mol Ecol* 18:1294–1305. <https://doi.org/10.1111/j.1365-294X.2009.04085.x>
33. Ramond E, Maclachlan C, Clerc-Rosset S, Knott GW, Lemaître B. 2016. Cell division by longitudinal scission in the insect endosymbiont *Spiroplasma poulsonii*. *mBio* 7:e00881-16. <https://doi.org/10.1128/mBio.00881-16>
34. Herren JK, Paredes JC, Schüpfer F, Arafah K, Bulet P, Lemaître B. 2014. Insect endosymbiont proliferation is limited by lipid availability. *Elife* 3:e02964. <https://doi.org/10.7554/eLife.02964>
35. Herren JK, Paredes JC, Schüpfer F, Lemaître B. 2013. Vertical transmission of a *Drosophila* endosymbiont via cooption of the yolk transport and internalization machinery. *mBio* 4:e00532-12. <https://doi.org/10.1128/mBio.00532-12>
36. Harumoto T, Lemaître B. 2018. Male-killing toxin in a bacterial symbiont of *Drosophila*. *Nature* 557:252–255. <https://doi.org/10.1038/s41586-018-0086-2>
37. Harumoto T. 2023. Self-stabilization mechanism encoded by a bacterial toxin facilitates reproductive parasitism. *Curr Biol* 33:4021–4029. <https://doi.org/10.1016/j.cub.2023.08.032>
38. Paredes JC, Herren JK, Schüpfer F, Marin R, Claverol S, Kuo CH, Lemaître B, Béven L. 2015. Genome sequence of the *Drosophila melanogaster* male-killing *Spiroplasma* strain MSRO endosymbiont. *mBio* 6:e02437-14. <https://doi.org/10.1128/mBio.02437-14>
39. Masson F, Calderon Copete S, Schüpfer F, Garcia-Arreaez G, Lemaître B. 2018. *In vitro* culture of the insect endosymbiont *Spiroplasma poulsonii* highlights bacterial genes involved in host-symbiont interaction. *mBio* 9:e00024-18. <https://doi.org/10.1128/mBio.00024-18>
40. Masson F, Schüpfer F, Jollivet C, Lemaître B. 2020. Transformation of the *Drosophila* sex-manipulative endosymbiont *Spiroplasma poulsonii* and persisting hurdles for functional genetic studies. *Appl Environ Microbiol* 86:e00835-20. <https://doi.org/10.1128/AEM.00835-20>
41. Shokal U, Yadav S, Atri J, Accetta J, Kenney E, Banks K, Katakam A, Jaenike J, Eleftherianos I. 2016. Effects of co-occurring *Wolbachia* and *Spiroplasma* endosymbionts on the *Drosophila* immune response against insect pathogenic and non-pathogenic bacteria. *BMC Microbiol* 16:16. <https://doi.org/10.1186/s12866-016-0634-6>
42. Herren JK, Lemaître B. 2011. *Spiroplasma* and host immunity: activation of humoral immune responses increases endosymbiont load and susceptibility to certain gram-negative bacterial pathogens in *Drosophila melanogaster*. *Cell Microbiol* 13:1385–1396. <https://doi.org/10.1111/j.1462-5822.2011.01627.x>
43. Marra A, Masson F, Lemaître B. 2021. The iron transporter Transferrin 1 mediates homeostasis of the endosymbiotic relationship between *Drosophila melanogaster* and *Spiroplasma poulsonii*. *Microlife* 2:uqab008. <https://doi.org/10.1093/femsm/luqab008>
44. Clemmons AW, Lindsay SA, Wasserman SA. 2015. An effector peptide family required for *Drosophila* toll-mediated immunity. *PLoS Pathog* 11:e1004876. <https://doi.org/10.1371/journal.ppat.1004876>
45. Schwenke RA, Lazzaro BP, Wolfner MF. 2016. Reproduction–immunity trade-offs in insects. *Annu Rev Entomol* 61:239–256. <https://doi.org/10.1146/annurev-ento-010715-023924>
46. Iatsenko I, Marra A, Boquete JP, Peña J, Lemaître B. 2020. Iron sequestration by transferrin 1 mediates nutritional immunity in *Drosophila melanogaster*. *Proc Natl Acad Sci U S A* 117:7317–7325. <https://doi.org/10.1073/pnas.1914830117>
47. Hrdina A, Iatsenko I. 2022. The roles of metals in insect–microbe interactions and immunity. *Curr Opin Insect Sci* 49:71–77. <https://doi.org/10.1016/j.cois.2021.12.004>
48. Shaka M, Arias-Rojas A, Hrdina A, Frahm D, Iatsenko I. 2022. Lipopolysaccharide-mediated resistance to host antimicrobial peptides and hemocytederived reactive-oxygen species are the major *Providencia alcalifaciens* virulence factors in *Drosophila melanogaster*. *PLoS Pathog* 18:e1010825. <https://doi.org/10.1371/journal.ppat.1010825>
49. Dudzic JP, Hanson MA, Iatsenko I, Kondo S, Lemaître B. 2019. More than black or white: melanization and toll share regulatory serine proteases in *Drosophila*. *Cell Rep* 27:1050–1061. <https://doi.org/10.1016/j.celrep.2019.03.101>
50. Simhadri RK, Fast EM, Guo R, Schultz MJ, Vaisman N, Ortiz L, Bybee J, Slatko BE, Frydman HM. 2017. The gut commensal microbiome of *Drosophila melanogaster* is modified by the endosymbiont *Wolbachia*. *mSphere* 2:e00287-17. <https://doi.org/10.1128/mSphere.00287-17>
51. Issa N, Guillaumot N, Lauret E, Matt N, Schaeffer-Reiss C, Van Dorselaer A, Reichhart J-M, Veillard F. 2018. The circulating protease persephone is an immune sensor for microbial proteolytic activities upstream of the *Drosophila* toll pathway. *Mol Cell* 69:539–550. <https://doi.org/10.1016/j.molcel.2018.01.029>
52. Buchon N, Poidevin M, Kwon H-M, Guillou A, Sottas V, Lee B-L, Lemaître B. 2009. A single modular serine protease integrates signals from pattern-recognition receptors upstream of the *Drosophila* toll pathway. *Proc Natl Acad Sci U S A* 106:12442–12447. <https://doi.org/10.1073/pnas.0901924106>
53. Allen KJ, Gurrin LC, Constantine CC, Osborne NJ, Delatycki MB, Nicoll AJ, McLaren CE, Bahlo M, Nisselle AE, Vulpe CD, Anderson GJ, Southey MC, Giles GG, English DR, Hopper JL, Olynyk JK, Powell LW, Gertig DM. 2008. Iron-overload-related disease in HFE hereditary hemochromatosis. *N Engl J Med* 358:221–230. <https://doi.org/10.1056/NEJMoa073286>
54. Alvear VMH, Mateos M, Cortez D, Tamborindeguy C, Martinez-Romero E. 2021. Differential gene expression in a tripartite interaction: *Drosophila*, *Spiroplasma* and parasitic wasps. *PeerJ* 9:e11020. <https://doi.org/10.7717/peerj.11020>
55. Gerth M, Martinez-Montoya H, Ramirez P, Masson F, Griffin JS, Aramayo R, Siozios S, Lemaître B, Mateos M, Hurst GDD. 2021. Rapid molecular evolution of *Spiroplasma* symbionts of *Drosophila*. *Microb Genom* 7:1–15. <https://doi.org/10.1099/mgen.0.000503>
56. De Gregorio E, Spellman PT, Rubin GM, Lemaître B. 2001. Genome-wide analysis of the *Drosophila* immune response by using oligonucleotide microarrays. *Proc Natl Acad Sci U S A* 98:12590–12595. <https://doi.org/10.1073/pnas.221458698>
57. Kremer N, Voronin D, Charif D, Mavingui P, Mollereau B, Vavre F. 2009. *Wolbachia* interferes with ferritin expression and iron metabolism in

- insects. *PLoS Pathog* 5:e1000630. <https://doi.org/10.1371/journal.ppat.1000630>
58. Arias-Rojas A, Frahm D, Hurwitz R, Brinkmann V, Iatsenko I. 2023. Resistance to host antimicrobial peptides mediates resilience of gut commensals during infection and aging in *Drosophila*. *Proc Natl Acad Sci U S A* 120:e2305649120. <https://doi.org/10.1073/pnas.2305649120>
59. Iatsenko I, Boquete J-P, Lemaitre B. 2018. Microbiota-derived lactate activates production of reactive oxygen species by the intestinal NADPH oxidase Nox and shortens *Drosophila* LifeSpan. *Immunity* 49:929–942. <https://doi.org/10.1016/j.immuni.2018.09.017>
60. Pfaffl MW. 2001. A new mathematical model for relative quantification in real-time RT-PCR. *Nucleic Acids Res* 29:e45. <https://doi.org/10.1093/nar/29.9.e45>
61. Robinson MD, Oshlack A. 2010. A scaling normalization method for differential expression analysis of RNA-seq data. *Genome Biol* 11:1–9. <https://doi.org/10.1186/gb-2010-11-3-r25>
62. Love MI, Huber W, Anders S. 2014. Moderated estimation of fold change and dispersion for RNA-Seq data with DESeq2. *Genome Biol* 15:550. <https://doi.org/10.1186/s13059-014-0550-8>
63. Lyne R, Smith R, Rutherford K, Wakeling M, Varley A, Guillier F, Janssens H, Ji W, McLaren P, North P, Rana D, Riley T, Sullivan J, Watkins X, Woodbridge M, Lilley K, Russell S, Ashburner M, Mizuguchi K, Micklem G. 2007. FlyMine: an integrated database for *Drosophila* and *Anopheles* genomics. *Genome Biol* 8:1–16. <https://doi.org/10.1186/gb-2007-8-7-r129>